

SUPPLEMENTAL MATERIALS:

Table of Contents:

<u>Supplemental Methods</u>	Pages 2-4
<u>Supplemental Analyses</u>	Page 5
<u>Supplemental Tables 1-10</u>	Pages 6-9
<u>Supplemental Figures 1-3</u>	Pages 10-12

Supplemental Methods:

CD31 Workflow

QuPath-0.2.3, an open source software platform for digital pathology and WSI image analysis, was used for data extraction from CD31 slides. HistoQC software was downloaded from github using this repository, <https://github.com/choosehappy/HistoQC>.

Segmentation: Annotations and Nuclei Detection

To initiate feature discrimination, the WSIs stained with CD31 were imported into a new QuPath project. The following steps were completed using Apache Groovy scripts.

- a) Preprocessing
- b) Annotation
- c) Nuclei detection

Preprocessing

Preprocessing included setting the image type (Brightfield H-DAB), background, and stain deconvolution. These were the parameters used:

```
setColorDeconvolutionStains({'Name' : "H-DAB CD31",  
    "Stain 1" : "Hematoxylin", "Values 1" : "0.59666 0.75249 0.27885 ",  
    "Stain 2" : "DAB", "Values 2" : "0.24042 0.48171 0.84271 ",  
    "Background" : " 235 235 243 "});
```

Annotation

The following pixel classifiers and their corresponding parameters were generated in order to annotate specific regions or features of interest within the annotated ROI. Resolution parameters may differ based on the slides.

- a. A Region of Interest (ROI) was annotated using a pixel classifier and classified as “CD31ROI”. The following threshold values were used: *Resolution: Low (4.02 $\mu\text{m}/\text{px}$), Channel: Average, Prefilter: Gaussian, Smoothing Sigma: 4, Threshold: 231, Minimum object size: 4000 μm^2 , and Minimum hole size: 4000 μm^2 .*
- b. CD31Tissue_classifier_v3: *Resolution: Very High (0.50 $\mu\text{m}/\text{px}$), Channel: Average, Prefilter: Gaussian, Smoothing Sigma: 4, Threshold: 235, Minimum object size: 10 μm^2 , and Minimum Hole Size: 10 μm^2 .*
- c. CD31DAB_classifier_v3: *Resolution: Full (0.25 $\mu\text{m}/\text{px}$), Channel: DAB, Prefilter: Gaussian, Smoothing Sigma: 1.5, Threshold: 0.2, Minimum object size: 10 μm^2 , and Minimum Hole Size: 10 μm^2*
- d. CD31HEMA_classifier_v3: *Resolution: Full(0.25 $\mu\text{m}/\text{px}$), Channel: Hematoxylin, Prefilter: Gaussian, Smoothing Sigma: 1.5, Threshold: 0.2, Minimum object size: 10 μm^2 , and Minimum Hole Size: 10 μm^2*

Nuclei Detection

Having classified the annotations, positive cell detection was run with the following parameters on the “CD31 Tissue” annotations. Supplemental Figure S.1 defines the parameters used for running positive cell detection. The annotation and nuclei data was exported as GeoJSON files for each WSI. Each WSI file therefore has a corresponding nuclei.json file and annotation.json file.

Extracting Features

The corresponding nuclei and annotation GeoJSON files were then opened using Python's Geojson and Shapely libraries. Areas for tissue, DAB, hematoxylin, and nuclei were calculated using the Shapely library and collected in four respective Pandas dataframes. The four data frames were then saved to tis.csv, dab.csv, hem.csv, and nuc.csv. Each of these files contain the cohort, filename, and area. In dab.csv, the corresponding Shapely polygons and polygon coordinates were also saved.

Binning and DAB dilation

Dab.csv was loaded in a pandas dataframe for DAB object area assessment and binning by size. Objects where DAB areas were in the top/bottom 0.1% were dropped to compensate for staining artifacts, off-target staining, and rare, sporadically distributed larger coronary vessels. The full distribution of DAB objects is presented in Supplemental Figure S.2, and summary statistics on the sizes of measured DAB objects is presented in Supplemental Table S.1.

Defining Boundaries for Various Binning Processes

1. Quartile bin boundaries were calculated using statistics from the csv dataframe for the 25th, 50th, and 75th percentiles.
2. Standard deviation bin boundaries were calculated by the addition of a new column to the data frame that holds the z-score for that row. The z-score was calculated using the equation $\frac{Area - Mean}{Standard\ Deviation}$. The boundaries were then defined as a) within ± 0.5 standard deviations from the mean b) within ± 1.0 standard deviation excluding the area between ± 0.5 standard deviations c) within ± 1.5 standard deviation excluding the area between ± 1.0 standard deviations d) within ± 2.0 standard deviation excluding the area between ± 1.5 standard deviations e) within ± 3.0 standard deviation excluding the area between ± 2.0 standard deviations f) outside of ± 3.0 standard deviations.
3. Biological bin boundaries were defined as shown in Supplemental Table S.2 (conversion used: area of 1 *pixel*² = 0.0633 μm^2).
4. Dab areas in the top 0.1% were classified as outliers and treated as a separate bin

DAB Dilation and Binning Process

The DAB dataframe was grouped by cohorts and filename. For each group, its corresponding nuc.json file was opened and its nuclei detections were read using shapely and geojson. Shapely's unary_union was used for dilating the DAB annotation, STRtree was used for searching nuclei centroids, and Shapely's Within function was used to identify nuclei within DAB. Nuclei that were within overlapping dilated regions were not double counted. The following process was performed by dilating the DAB annotation based on the bins. Supplemental Table S.3 outlines the bin dilation sizes.

- a. findNucsInDAB_qrt: identify nuclei that were within quartile boundaries
- b. findNucsInDAB_std: identify nuclei that were within standard deviation boundaries
- c. findNucsInDAB_bio: identify nuclei that were within biological boundaries
- d. findNucsInDAB_excl: identify nuclei that were within the excluded DAB boundaries

The final CD31 results were collected and saved to CSV.

Movats Workflow

Movat's Pentachrome classification started with extracting 2000 x 2000 tiles from the WSI.

Segmentation

Movat's Pentachrome stained tiles included regions of myocytes, collagen, basement membrane, stroma, and nuclei. Supplemental Table S.3 presents each of these features, their corresponding color, and the threshold range used.

Tiled images were opened in the BGR color space using OpenCV and a Gaussian blur with a 5 x 5 kernel was applied to this image. A low pass filter, gaussian kernel, was applied in order to reduce random noise in the tiled images. This Gaussian blurred image was then converted to HSV. Feature detection in the HSV space was chosen because BGR includes luminance which makes feature discrimination difficult. HSV abstracts hue while separating illumination making it better suited for feature detection. Each stained feature correlated with a specific range of colors in HSV space defined in Supplemental Table S.4.

However, certain slides were overstained and this created issues with the segmentation process which would lead to false positives for stromal detections. To address this, overstained images were manually identified and brightened using Python's OpenCV `convertScaleAbs` with an alpha (contrast) value of 1.5 and a beta (brightness) value of 0 prior to segmentation.

Binary masks of each color's minimum and maximum range were created. Before calculating the area of the binary masks, post processing using Skimage's morphology functions was needed to reduce noise. The following Supplemental Table S.5 describes the various morphological parameters used. A myocardium mask was also generated by filling holes in the myocyte mask and dilating it until large sheets of myocytes were confluent.

Feature Quantification

After morphology functions were applied, Python's NumPY was used to calculate the total area for each binary mask, where each binary mask was represented by a specific feature. The features were summed by WSI file and grouped by cohort. This Movats data was then saved to a CSV file.

Merging CD31 and Movats Data

CD31 and Movats data was merged using Pandas based on corresponding filenames. From this combined dataset, the final set of n=680 features for morphologic model construction were generated. This involved using the extracted parameters as detailed above to calculate different cell/nuclei, tissue-type, and DAB object ratios to assess normalized densities and areas-covered in different parts of the digital slides. Specific examples of generated features can be found in the multivariate results in Supplemental Tables S.8 and S.9 below. A complete list of features is available upon reasonable request.

Supplemental Analyses:

Assessing Established Predictive Clinical Risk Factors for CAV:

The starting point for ClinCAV-Pr Model development and optimization was not a traditional ‘empty’ (containing no variables) or ‘full’ (containing all variables) model. Instead, we chose to start with predictive risk factors recently established in a large, multicenter observational study on CAV trajectories (manuscript reference 5). These risk factors – donor age, donor sex, donor cigarette use, recipient LDL cholesterol at 1-year post transplant, presence of +DSA at 1-year, and history of cellular rejection at 1-year – were used to develop and test a model as described in the statistical methods section. As shown in Supplemental Figure S.3, this ‘proven risk factor’ model fairly poorly overall, with an AUROC of 0.63 and an accuracy of 62%. This poor performance justified the additional feature selection steps employed to develop the final ClinCAV-Pr in used in this experiment (see main manuscript), which utilizes several of these previously established risk factors while also adding additional risk factors describing histology/rejection history and donor/recipient medical history.

HistoCAV-Pr Model Performance by ISHLT Grade:

Recognizing that there was a baseline imbalance between No-CAV and PrE-CAV groups in the proportion of EMBs with OR vs. 1R rejection grades (no-CAV: 57.8% 1R grade, while PrE-CAV 76% 1R grade), we explored whether model predictions were strongly associated with underlying ISHLT grade. Supplemental Table S.6 shows that misclassifications by the HistoCAV-Pr Model were overall fairly balanced between grades, with a 13.3% (8/60) misclassification rate for OR EMBs, and a 16.7% misclassification rate for 1R EMBs ($p=0.59$). Looking more closely, ISHLT grade does not significantly impact misclassification rates within or between the No-CAV and PrE-CAV groups. This suggests that model performance is not significantly affected by underlying ISHLT grade, and that misclassified cases are unlikely to be the result of the underlying ISHLT grade.

Morphologic Model Performance by Slide Scanner Manufacturer:

While slide scanners are commonplace in pathology departments across the world, there are several different companies manufacturing these devices. Different manufacturers utilize different methods to create digital images, with differences in hardware (charge-coupled device chips vs. lighting bulbs) and software approaches (stitching vs. compression) potentially affecting final image appearance (manuscript reference 36). Prior literature has shown that these differences can potentially impact downstream image analysis pipeline performance. Therefore, we deliberately incorporated digitized slides from two different slide scanner devices in our study to permit an assessment of the resilience of the image analysis pipeline and subsequent models to variations in slide scanner technology. Digital images arising from each scanner were combined into a single cohort prior to randomization to training/test sets. As shown in Supplemental Table S.7, the overall classification performance (combining training and test set results) of both the HistoCAV-Dx and HistoCAV-Pr Models were unaffected by slide scanner manufacturer. Note that because training and test sets are combined for this analysis, the overall AUROC and accuracy are designed to reflect only overall differences in performance between slide scanners, and not overall validated model performance (as presented in the primary Results).

Supplemental Tables:

Table S.1: Summary of DAB object sizes

	Size (μm^2)
Average DAB Object [standard deviation]	80.0 [± 90]
Median DAB Object	48.0
Quartile 1	10-24
Quartile 2	24-48
Quartile 3	48-95
Quartile 4	95-491

Table S.2: Biologically inspired boundary definitions.

Biological Bin Definitions/Boundaries	
Capillaries	$< 78.4\mu\text{m}^2$ ($< 10\mu$ in minor axis luminal diameter)
Small Precapillary Arterioles	$78.5 - 314\mu\text{m}^2$
Large Precapillary Arterioles	$315 - 1000\mu\text{m}^2$
Arterioles	$> 1000\mu\text{m}^2$
Large Outliers	99.9% cutoff

Table S.3: Binning strategies and their corresponding bin dilation sizes.

Quartile Bins		Standard Deviation Bins		Biological Bins	
Bin	Dilation (pixels)	Bin	Dilation (pixels)	Bin	Dilation (pixel)
q1	2 px	s1	2 px	b1	2 px
q2	5 px	s2	5 px	b2	5 px
q3	10 px	s3	10 px	b3	10 px
q4	15 px	s4	15 px	b4	15 px
		s5	20 px	b5	20 px
		s6	25 px		

Table S.4: Movats features, their corresponding colors, and the threshold range used.

Feature	Color	Threshold Range
Myocyte	Red	$L_RED_MIN = np.array([0,20,70])$ $L_RED_MAX = np.array([5,255,255])$ $U_RED_MIN = np.array([140,20,70])$ $U_RED_MAX = np.array([180,255,255])$
Collagen	Yellow	$YELLOW_MIN = np.array([5, 20, 70],)$ $YELLOW_MAX = np.array([60, 255, 255])$
Basement Membrane	Blue	$BLUE_MIN = np.array([60, 20, 70],)$ $BLUE_MAX = np.array([140, 255, 255])$
Stroma and Nuclei	Black	$BLACK_MIN = np.array([1,1,1])$ $BLACK_MAX = np.array([255,255,70])$
Background	White	$WHITE_MIN = np.array([0, 0, 180])$ $WHITE_MAX = np.array([255,60, 255])$

Table S.5: Parameters for morphological masks.

Color (Feature)	Post Processing Values
Red (Myocyte)	<code>binary_erosion(boolean_mask, disk(3))</code> <code>remove_small_objects(boolean_mask, min_size=400)</code> <code>remove_small_holes(boolean_mask, 400)</code>
Yellow (Collagen)	<code>binary_dilation(boolean_mask, disk(3))</code> <code>remove_small_objects(boolean_mask, min_size=100)</code> <code>remove_small_holes(boolean_mask, 400)</code>
Blue (Basement Membrane)	<code>binary_dilation(boolean_mask, disk(3))</code> <code>remove_small_objects(boolean_mask, min_size=100)</code> <code>remove_small_holes(boolean_mask, 100)</code>
Black (Stroma and Nuclei)	<code>remove_small_objects(boolean_mask, min_size=100)</code> <code>remove_small_holes(boolean_mask, 5000)</code>
White (Background)	<code>binary_dilation(boolean_mask,(prev_mask), disk(3))</code> <code>remove_small_objects(boolean_mask, min_size=100)</code> <code>remove_small_objects(boolean_mask, min_size=100)</code> <code>remove_small_holes(boolean_mask, 5000)</code>
Myocardium	<code>binary_dilation(boolean_mask,(prev_mask), disk(30))</code> <code>remove_small_holes(boolean_mask, 5000)</code> <code>remove_small_objects(boolean_mask, min_size=5000)</code> <code>binary_erosion(boolean_mask, disk(20))</code>

Table S.6: Assessing the impact of differences in the underlying ISHLT grade of study biopsies used for future CAV prediction with the HistoCAV-Pr Model.

	% ISHLT Grade 0R biopsies Misclassified (n)	% ISHLT Grade 1R biopsies Misclassified (n)	p val (0R vs 1R)
No-CAV	10.4% (5/48)	17.6 (6/34)	0.34
PrE-CAV	25% (3/12)	15.8 (6/38)	0.47
p val (No-CAV vs PrE-CAV)	0.18	0.83	---

PrE-CAV = pre-early cardiac allograft vasculopathy (CAV) patients, defined as patients experiencing overt CAV by 5-years post-transplant but without diagnosis at 1-year. No-CAV = patients without overt CAV at 6-years post-transplant. ISHLT = international society for heart and lung transplantation

Table S.7: Performance of study Morphologic Models by slide scanner manufacturer.

Morphologic Model	Hamatsu S360		Aperio ScanScope		p value
	AUROC	Accuracy (n)	AUROC	Accuracy (n)	
HistoCAV-Dx Model	0.93	88.3% (68/77)	0.94	89.3% (50/56)	0.86
HistoCAV-Pr Model	0.88	84.8% (67/79)	0.90	84.9% (45/53)	0.99

Table S.8: Variables in HistoCAV-Dx Model for Diagnosing cardiac allograft vasculopathy, with annotated descriptions.

Variable	Variable Description	Multivariate p Value	Odds Ratio
prop_dab_nuc_in_q23	% of total vascular nuclei found within larger capillaries & small pre-capillary arterioles	0.002	0.806664
nuc_in_dab_by_myocard	# Nuclei within vasculature, normalized by myocyte area	0.023	0.581875
nuc_outside_by_myocard	# Nuclei outside the vascular/perivascular space, normalized by myocyte area	0.02	1.67034
nuc_dens_in_dilonly_by_myocard	% of total nuclei in perivascular space, normalized by myocyte area	0.007	0.883957
nuc_in_dab_by_stroma_in_myocard	# Nuclei within in vasculature, normalized by stromal area	0.039	1.555839
nuc_outside_by_stroma_in_myocard	# Nuclei outside the vasculature/perivascular space, normalized by stromal area	0.049	0.685748
total_stroma_by_myocard	Total stroma to myocardium ratio	0.033	0.474698
collagen_inmyocard_by_myocard	Collagen content of interstitium	0.001	1.4787
compstat1	% of vascular nuclei around larger capillaries and small pre-capillary arterioles, normalized by stromal area	0.043	1.086368
dab_area_by_perc_myocard_in_myocard	Total vascular density (vascular object area to myocardium area)	0.067	0.835601
stro_myocard_original	Interstitial stromal area	0.033	1.216634

Table S.9: Variables in HistoCAV-Pr for predicting future cardiac allograft vasculopathy, with annotated descriptions.

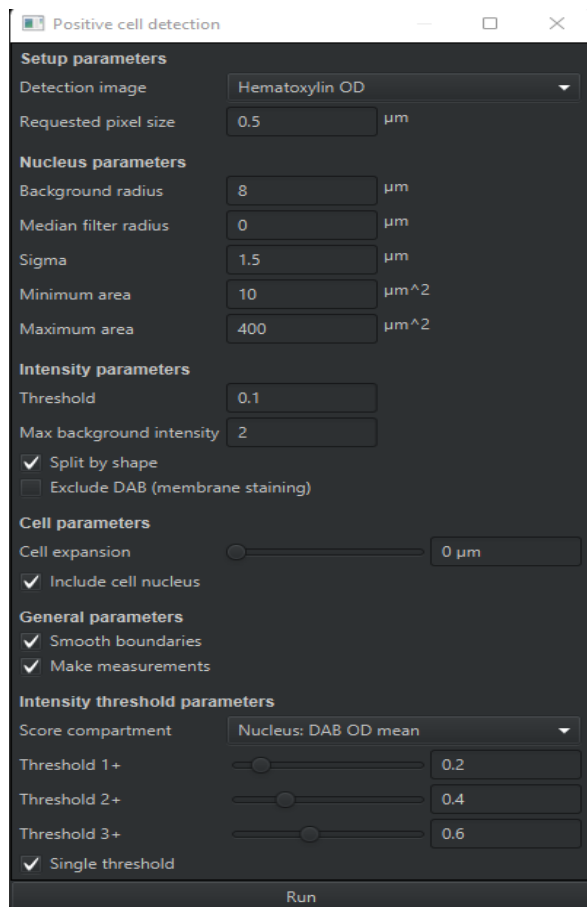
Variable	Variable Description	Multivariate p Value	Odds Ratio
stroma_in_myocard_by_myocard	Interstitial stroma, normalized by myocardial compartment size	0.006	1.711429
prop_dab_obj_in_dab_s234	% of microvessels that are capillaries or small pre-capillary arterioles	0.002	0.839721
white_in_myocard_by_myocard	Non-collagen/non-proteoglycan content of interstitium	0.047	0.860249
nuc_in_q34_dil_by_area_in_q34	# perivascular nuclei per unit vessel area for pre-capillary arterioles	0.004	1.204962
total_stroma_by_myocard	Total stroma to myocardium ratio	0.001	0.767723
prop_of_dab_area_in_dab_s56_	% of total vascular area comprised of larger pre-capillary arterioles	0.087	1.226093
dab_area_by_myocard	Total microvascular staining area, normalized by myocardium	0.008	2.998339
dab_s56_area_by_myocard	Total staining area of larger precapillary arterioles, normalized	0.008	1.562746
nuc_in_dildab_by_myocard	Total # of nuclei in and around vessels, normalized by myocard	0.016	0.405156
prop_dab_nuc_in_q2	% of total vascular nuclei found within capillaries	0.021	0.876805

Table S.10: Variables in an integrated ‘Histo-Clinical’ Model optimized through backwards elimination of variables from the final ClinCav-Pr and the final HistoCAV-Pr Model. Note that this multivariate model was not used as the final iCAV-Pr model due to inferior performance compared to a simple two-variable model using classification probabilities from ClinCAV-Pr and HistoCAV-Pr.

Variable	Variable Description	Multivariate p Value	Odds Ratio
stroma_in_myocard_by_myocard	Interstitial stroma, normalized by myocardial compartment size	0.045	2.30084
white_in_myocard_by_myocard	Non-collagen/non-proteoglycan content of interstitium	0.094	0.7725427
nuc_in_q34_dil_by_area_in_q34	# perivascular nuclei per unit vessel area for pre-capillary arterioles	0.025	1.339025
total_stroma_by_myocard	Total stroma to myocardium ratio	0.025	0.6811603
dab_area_by_myocard	Total microvascular staining area, normalized by myocardium	0.049	3.071829
dab_s56_area_by_myocard	Total staining area of larger precapillary arterioles, normalized	0.022	0.6394363
nuc_in_dildab_by_myocard	Total # of nuclei in and around vessels, normalized by myocard	0.044	0.2901358
prop_dab_nuc_in_q2	% of total vascular nuclei found within capillaries	0.032	0.7702914
History of Cellular Rejection	ISHLT grade 2R or 3R in first year post-transplant	0.052	1.358948
Recipient BMI	At 1-year post-transplant	0.025	1.157767
Donor Coronary Angiography Score	Derived from the Heart Donor Score, and incorporating donor age as a consideration	0.015	1.119375
Recipient Diabetes	With active treatment at 1-year post-transplant	0.098	1.021882

ISHLT = international society for heart and lung transplantation, BMI = body mass index, LDL= low density lipoprotein

Supplemental Figures:



The image shows a software window titled "Positive cell detection" with a dark theme. It contains several sections of parameters for cell detection:

- Setup parameters**
 - Detection image: Hematoxylin OD (dropdown)
 - Requested pixel size: 0.5 μm
- Nucleus parameters**
 - Background radius: 8 μm
 - Median filter radius: 0 μm
 - Sigma: 1.5 μm
 - Minimum area: 10 μm^2
 - Maximum area: 400 μm^2
- Intensity parameters**
 - Threshold: 0.1
 - Max background intensity: 2
 - ☒ Split by shape
 - ☐ Exclude DAB (membrane staining)
- Cell parameters**
 - Cell expansion: 0 μm (slider)
 - ☒ Include cell nucleus
- General parameters**
 - ☒ Smooth boundaries
 - ☒ Make measurements
- Intensity threshold parameters**
 - Score compartment: Nucleus: DAB OD mean (dropdown)
 - Threshold 1+: 0.2 (slider)
 - Threshold 2+: 0.4 (slider)
 - Threshold 3+: 0.6 (slider)
 - ☒ Single threshold

A "Run" button is located at the bottom right of the dialog.

Figure S.1: *Parameters outlined for running positive cell detection in QuPath.*

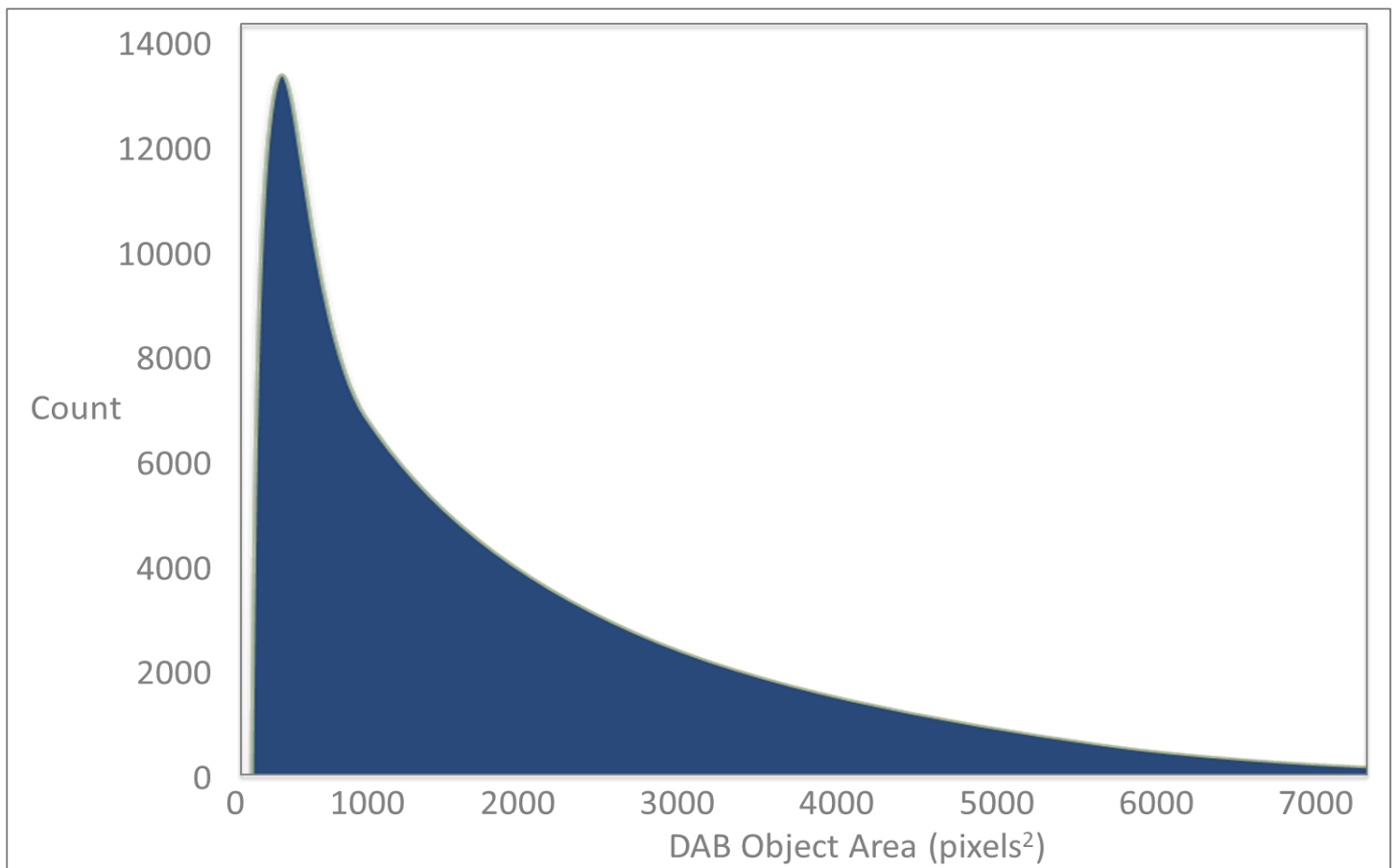


Figure S.2: Distribution of DAB object sizes: measured DAB object sizes (in pixels², with 1 pixel² = 0.0633μm²) and counts from final CD31 feature extraction workflow.

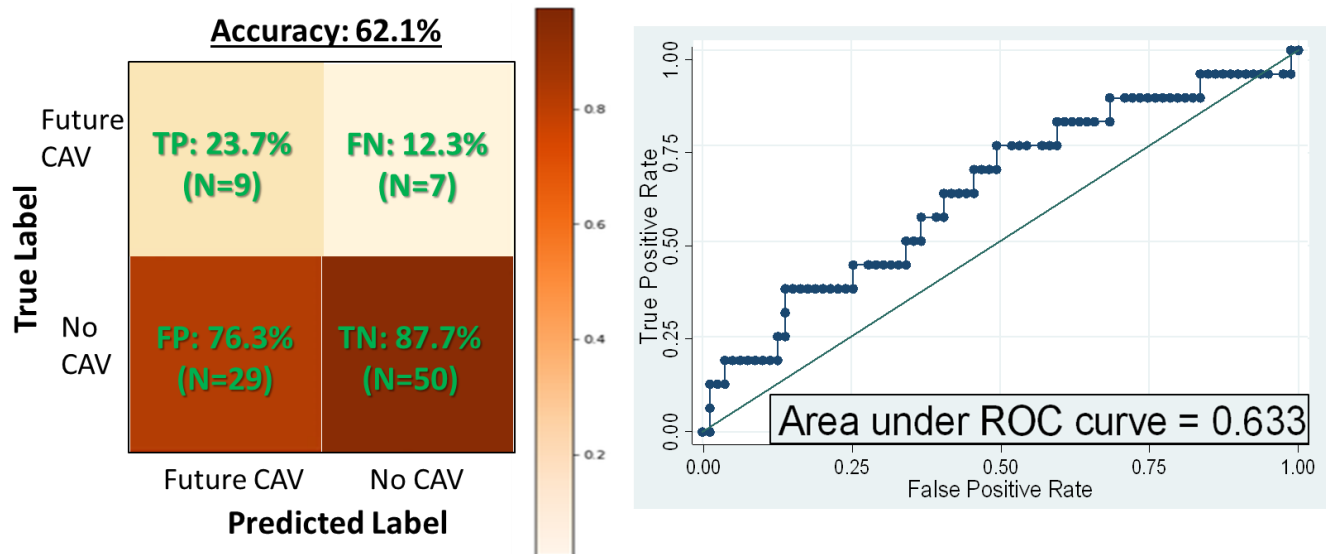


Figure S.3: Performance in the study test set of a clinical risk factor model using six previously validated multivariate predictors of cardiac allograft vasculopathy (CAV) trajectories. The overall performance of this six variable model is similar to but worse than the performance of the Clinical CAV Prediction Model (ClinCAV-Pr) developed in this experiment, which used several similar risk factors to those established in prior publications, along with several novel risk factors related to baseline patient risk for vasculopathy and/or coronary artery disease.